INTERNATIONAL JOURNAL FOR NUMERICAL METHODS IN FLUIDS
Int. J. Numer. Meth. Fluids 2005; **47**:1011–1018
Published online 31 January 2005 in Wiley InterScience (www.interscience.wiley.com). DOI: 10.1002/fld.928

Numerical simulation of an experimental gas–gas jet generated by single-hole diesel-like injection

O. El Ganaoui[1,*,†], C. Habchi[1], G. Bruneaux[1] and I. Danaila[2]

[1]*Institut Franais du Pétrole, 1 & 4 avenue de Bois Préau, 92852 Rueil-Malmaison, France*
[2]*Laboratoire Jacques-Louis Lions, Université Paris 6, 175 rue du Chevaleret, 75013 Paris, France*

SUMMARY

In this paper, we address the issue of accurate modelling of experimental data in order to provide numerical settings for Reynolds averaged Navier–Stokes (RANS) numerical simulation of the gas–gas jet generated by a single-hole diesel-like injector. Since experimental operating conditions usually do not document the inlet boundary conditions, both subsonic and supersonic inlets have been considered for the numerical simulation. For the supersonic case, a two-dimensional (2D) cartesian mesh has been used. For this case, good agreement with experimental jet penetration is obtained when realistic time evolution of the inlet pressure is prescribed but the jet shape is different compared to the experimental one. For the subsonic case, the axisymmetric RANS simulation allows to obtain the best agreement between experimental and numerical jet penetrations, head jet shapes and fuel density profiles. Copyright © 2005 John Wiley & Sons, Ltd.

KEY WORDS: IFP-C3D RANS code; gas–gas jet

1. INTRODUCTION

To face the stringent emission standard motivated by environmental issues, the automotive industry is continuously upgrading the engine technologies. One of the main innovations in the last few years is high pressure direct injection (HPDI) that has already proven its capacity to reduce soot and NO_x emissions of diesel engines. In modern multidimensional (3D) CFD codes such as IFP-C3D [1], the spray results may be very sensitive to the grid size and injection initial conditions. The purpose of this paper is to determine in which numerical conditions (*grid size*, *inlet boundary conditions*, *etc*) spray simulations have to be achieved in order to improve the accuracy of CFD code results. We have chosen to use available quantitative density images carried out by Bruneaux [2] on a fuel (methane CH_4) jet using laser-induced fluorescence (LIF). The main features of this experiment are given in

*Correspondence to: O. El Ganaoui, PSA Peugeot Citroén, 18 rue des Fauvelles, 92250 La Garenne Colombes, France.
†E-mail: ouafae.elganaoui@club-internet.fr, ouafae.elganaoui@mpsa.com

Received 27 April 2004
Revised 21 December 2004
Accepted 21 December 2004

the following section. Next, the IFP-C3D code is briefly described. The computational meshes and boundary conditions are presented, followed by the discussion of the numerical sensitivity study carried out.

2. DESCRIPTION OF EXPERIMENTS

This numerical study is based on the experiments performed by Bruneaux [2] who carried out quantitative fuel (methane CH_4) density visualizations using the LIF technique (Figure 1). Measurements are performed in a high-pressure cell where the CH_4 gaseous jet is injected into nitrogen (N_2) using a single-hole nozzle. Experimental data provide under three operating conditions (Table I) instantaneous and averaged images of jet CH_4 density for several instants during the injection process. Each image was normalized by the ratio of the calculated volume integrated intensity and the injected mass. The latter was determined from the mass flow rate equation, with the sonic diameter evolution characterized using a section calibration test [2]. In the resulting images, the intensity level is therefore directly proportional to the fuel density. Three instantaneous CH_4 density distribution and the averaged jet obtained using 100 realizations at $t = 1.25$ ms after start of injection (ASOI) are shown in Figure 2 for operating condition 3. This condition has been chosen for all the numerical simulations presented in this paper.

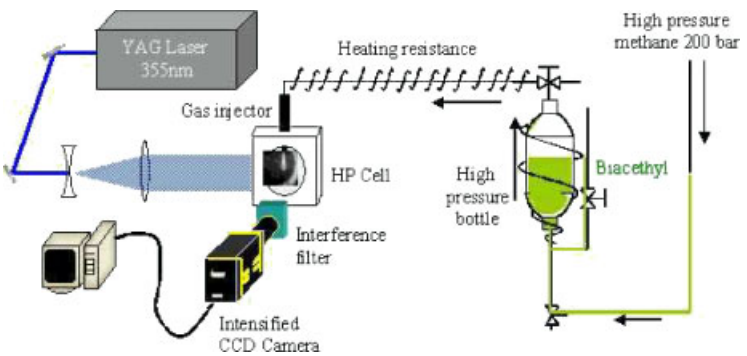

Figure 1. Experimental set-up for LIF imaging of methane jet using biacethyl tracer.

Table I. Operating conditions for the diesel-like injection.

Case	ρ_{cell} (kg m^{-3})	P_{cell} (MPa)	P_{inj} (MPa)	ρ_{inj} (kg m^{-3})	Q (g s^{-1})	Mach
1	25	2.7	15	79.5	4	1.5
2	12	1.3	15	79.5	4	1.5
3	25	2.7	11	58.3	3	1.42

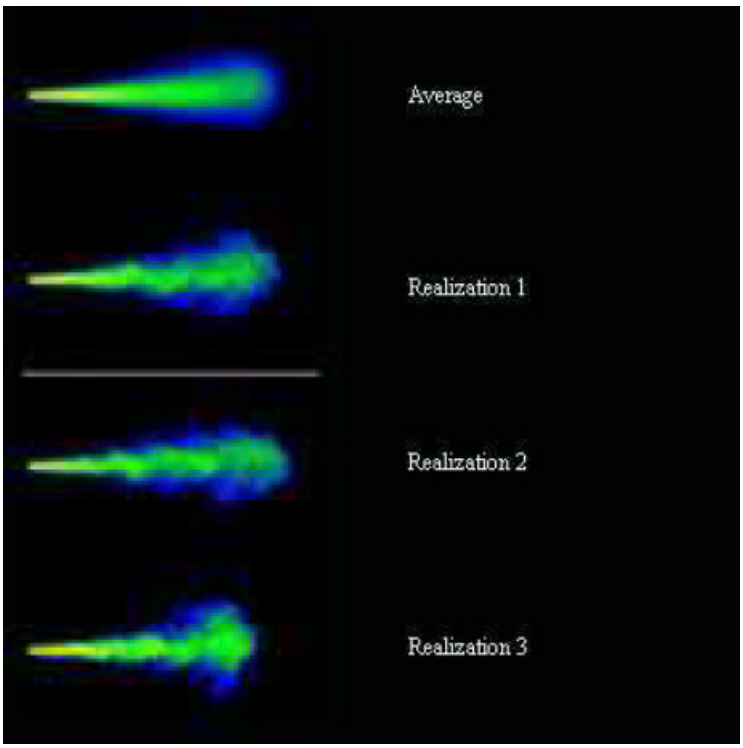

Figure 2. Comparison of mean and instantaneous images of fuel mass concentration for condition 3 at $t = 1.25$ ms.

3. THE IFP-C3D CODE

For the presented simulations, we used the IFP-C3D Reynolds averaged Navier–Stokes (RANS) code, which is currently developed at IFP for compressible flow computations, especially for internal combustion engines. It is a hexahedral finite volume unstructured parallel code. The code includes several numerical algorithms like time splitting, the SIMPLE iterative method, explicit subcycled convection and models like the $k - \varepsilon$ [3, 4] for turbulence and a Lagrangian description for the liquid spray. The equations are solved in three phases: source terms, diffusion and convection phase, respectively [1, 5]. It uses an arbitrary Lagrangian Eulerian (ALE) method to compute gas flows on moving grids.

4. COMPUTATIONAL MESHES AND BOUNDARY CONDITIONS

Two-dimensional (2D) and axisymmetrical meshes representing a cut passing through the nozzle hole are considered for the computations (Figure 3). In addition to the high pressure cell, a 20-mm part of the injection nozzle hole is included in the mesh. The injector nozzle hole diameter is 0.5 mm. Particular attention was paid to estimate numerical inflow boundary conditions from experimental data. From Table I one can notice that the cell pressure is

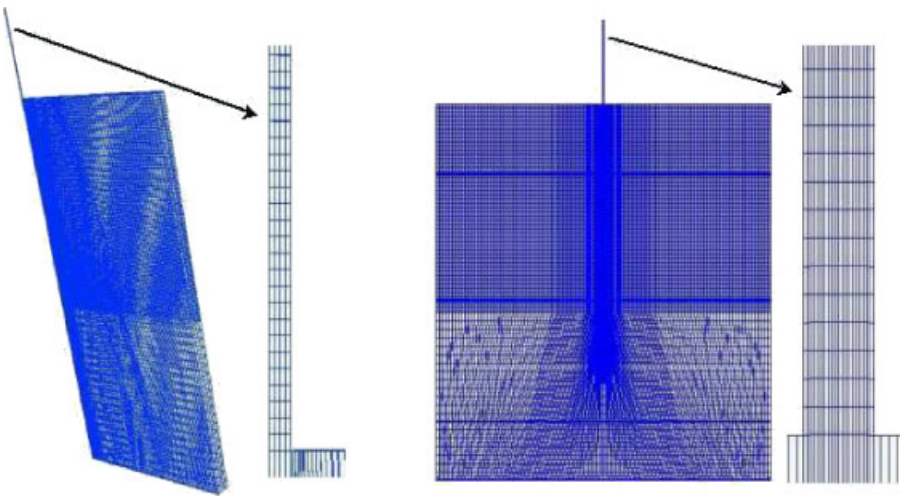

Figure 3. Axisymmetric mesh (left) and two-dimensional mesh (right).

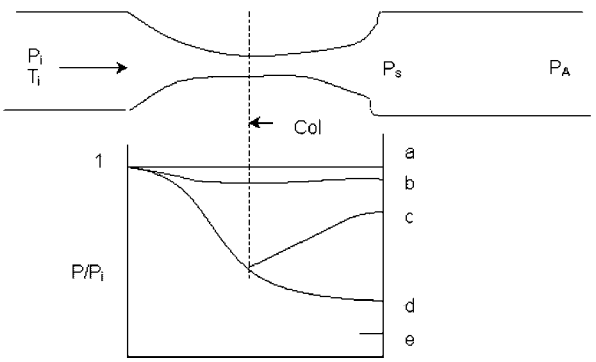

Figure 4. Pressure variation in convergent–divergent channel.

always smaller than the critical pressure (P_{cr}) given by $P_{cr} = P_{inj}(2/\gamma + 1)^{\gamma/(\gamma-1)}$, where P_{inj} is the injection pressure and γ is the ratio of specific heats. The injection is therefore operated under sonic conditions. Then we have assumed that the flow inside the nozzle is similar to the flow inside a convergent–divergent channel (Figure 4). Subsequently, we have determined the sonic diameter and the corresponding Mach number. The last column of Table I summarizes the calculated Mach number in the divergent channel. As it is difficult to know the shock wave position in the nozzle hole, the flow at the numerical inlet boundary (*which was chosen* 20 mm *from the hole exit*) may be subsonic or supersonic. Therefore, both cases are studied in the following.

4.1. Supersonic BC computations

If the flow is assumed to be supersonic in the hole (see curve 'd' in Figure 4), the shock wave would appear near the entry of the high-pressure cell. Consequently, the pressure has been

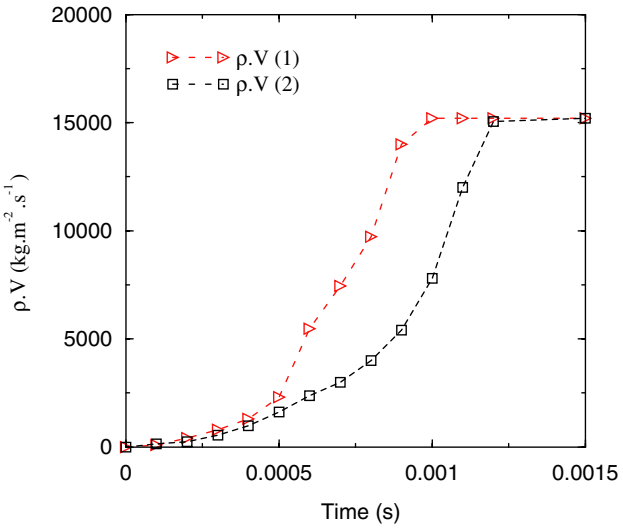

Figure 5. Flow rate used for simulation.

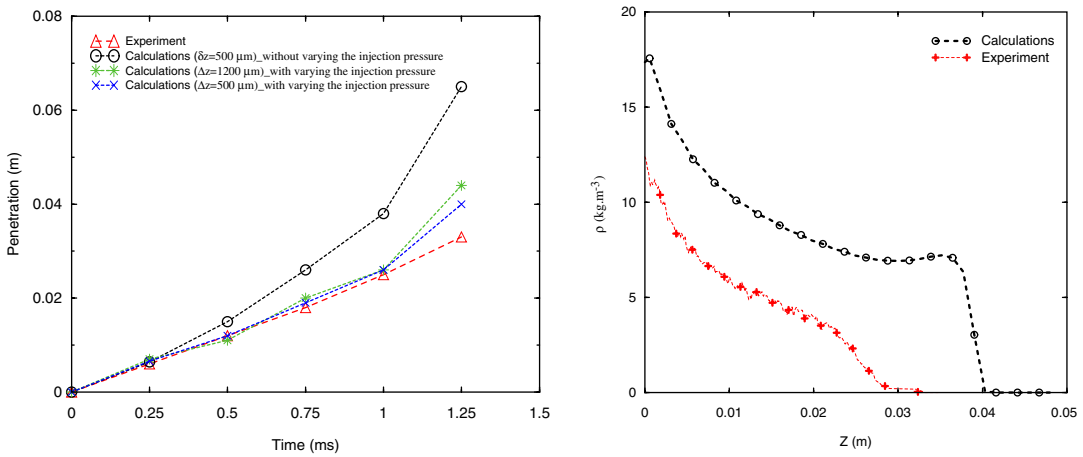

Figure 6. Comparisons of the jet penetration (left) and the fuel concentration (right) between calculations and measurements.

specified as a complementary boundary condition in the IFP-C3D code [8]. Following classical aerodynamic relationships [6], we can prescribe inflow boundary conditions $(\rho V, P, T, Y_i)$ using the experimentally given flow rate: $Q = \rho^* c^* S^*$, where $(*)$ indicates the sonic section parameters and Y_i is the i species concentration. The flow rate is experimentally given and shown in Figure 5 (curve $\rho.V(1)$).

Computation using constant inlet pressure led to poor agreement with experimental results (*see Figure 6 (left) for the penetration length*). We therefore had to take into account more realistic transient conditions for the specified pressure. As the experiments show that the critical diameter grows with the injector's needle lift, all the inlet conditions have been estimated

as a function of the injection time. Moreover, a more realistic inlet pressure is obtained if we take into account the pressure loss due to the needle opening. If we consider a needle of simple conical shape, the pressure loss may be estimated using the following relationship [7]:

$$\Delta P = \zeta \tfrac{1}{2} \rho V^2 \quad \zeta = 0.6 + \frac{0.15}{(h/D_0)^2} \tag{1}$$

where h is the needle lift, V the inlet velocity and D_0 the nozzle diameter. In order to assess the mesh sensitivity, two supersonic BC calculations have been carried out using two different Cartesian meshes. The first mesh has a $\Delta z = 1200\,\mu\text{m}$ and the second $\Delta z = 500\,\mu\text{m}$. The two meshes have the same spacing $\Delta x = 25\,\mu\text{m}$ inside the injection nozzle hole. The maximum time step allowed was set equal to $\Delta t = 0.1\,\mu\text{s}$ for the two computations. Figure 6 (left) shows a good agreement in terms of CH_4 jet penetration during the injection process except for the last calculated time ($t = 1.25\,\text{ms}$) when a small over-prediction of the penetration is obtained. It seems that the vertical cell height near the jet axis has a significant influence on the gas entrainment, fuel penetration and on the jet head shape. The computed symmetrical mushroom shape of the jet head indicates the existence of flow recirculations. This explains why it appears larger than in experiments (Figure 8). On the other hand, Figure 6 (right) shows a large difference between the computed and the experimental axial density profile. This disagreement suggests that Cartesian mesh used for the computations is not appropriate for the round jet simulations. In the next section, computations using an axisymmetric mesh are presented.

4.2. Subsonic BC computations

The shock wave is assumed to be located upstream the numerical inlet boundary. The flow is then subsonic in the whole computational domain (see curve 'c' in Figure 4). Therefore, the number of inlet boundary conditions is equal to that of dependent problem parameters minus one. For this case, the inlet pressure is determined using a numerical extrapolation from the inside of the computational domain.

For all the computation of this section, an axisymmetrical mesh has been used. Again a sensitivity study of the grid influence on the numerical results has been carried out. Figure 7 (left) shows that at least four cells in the nozzle hole are needed to reach grid convergence. The mushroom shape of the jet head has disappeared and the jet shape looks like the experimental one (Figure 8). Moreover, a better agreement between calculations and experiments in terms of axial density profiles than for the Cartesian mesh is obtained. Finally, Figure 7 (right) shows that using a second flow rate (curve $\rho.V(2)$ in Figure 5), the jet penetration and axial density profiles are closer to experimental ones. This second flow rate is calculated assuming that the needle level is slower than the needle level recorded in the experimentation.

5. CONCLUSIONS

In order to improve the accuracy of diesel spray numerical results, several gas–gas jet computations have been carried out using the IFP-C3D code. The initial injection parameters sensitivity study has shown that realistic and adequate transient inlet boundary conditions are needed to achieve good agreement between calculation and experiments. The mesh sensitivity

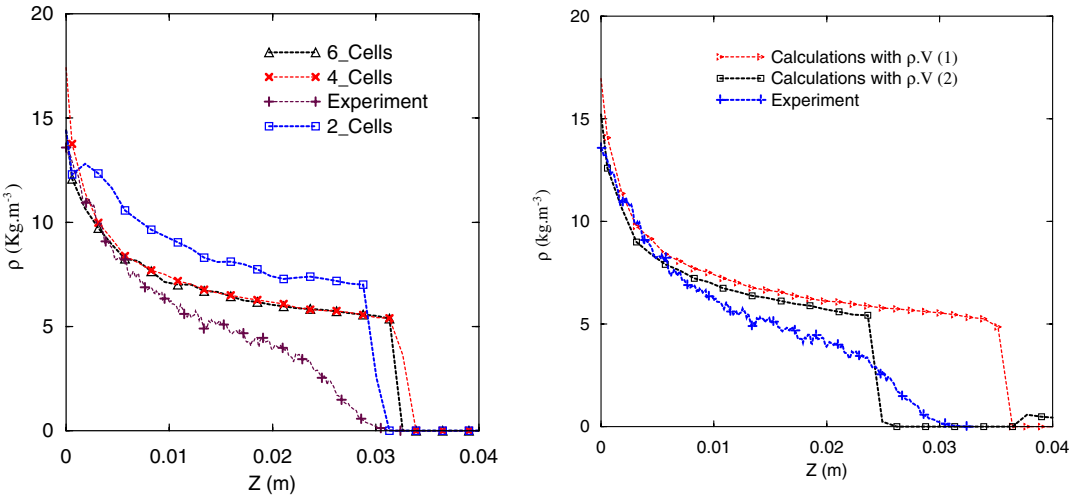

Figure 7. Sensitivity to the meshing for the fuel concentration (left) and sensitivity of the fuel concentration to the injected flow (right).

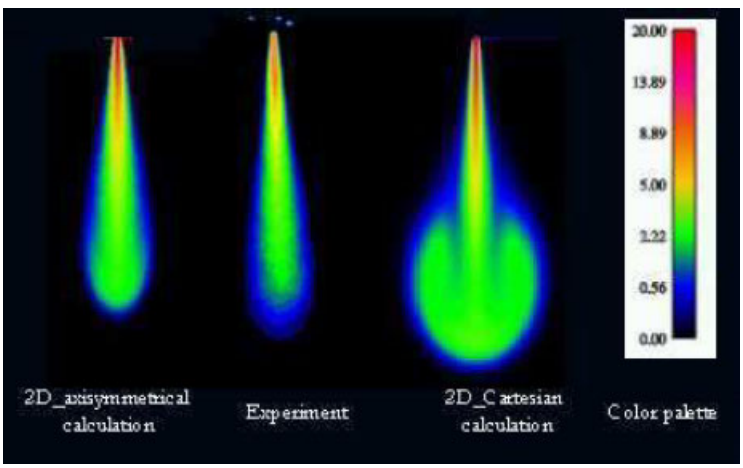

Figure 8. Fuel visualization compared to the experiment.

study has also shown that good jet head shape, penetration, and axial fuel density profiles can be obtained using an axisymmetrical mesh, and at least four cells inside the nozzle hole.

ACKNOWLEDGEMENTS

The authors gratefully acknowledge the support of Marc Zolver, Olivier Laget and Benjamin Réveillé from IFP.

REFERENCES

1. Zolver M, Klahr D, Torres A. An unstructured parallel solver for engine intake and combustion stroke simulation. *SAE Technical Paper*, 2002.
2. Bruneaux G. A study of mixture formation in direct injection diesel like conditions using quantitative fuel concentration visualizations in a gaseous fuel jet. *SAE Technical Paper*, 2002.
3. Schiestel R. *Modélisation et simulation des écoulements turbulents*. Hermes: Paris, 1993.
4. Cousteix J. *Turbulence et couche limite*. Cepadues: Toulouse, 1989.
5. Zolver M, Klahr D, Bohbot J, Laget O, Torres A. Reactive CFD in engines with a new unstructured parallel solver. *Gas Science and Technology-Rev. IFP* 2003; **58**:33–46.
6. Comolet R. *Mécanique expérimentale des fluides*, vol. 1(5). Masson: Paris, 1990.
7. Idel'cik IE. *Memento des pertes de charge*. Eyrolles: Paris, 1986.
8. Habchi C. *Contribution la simulation numérique d'un moteur deux temps*. University of Paris, 1990.

